

- Society, Dalton Transaction*, 1282-8 (1978).
6. V. B. Pett, L. L. Diaddario, E. R. Dockal, P. W. Corfield, C. Cecarelli, M. D. Ochrymowycz, and D. B. Rorabacher, *Inorganic Chemistry*, **22**, 3661-70 (1983).
 7. J. M. Desper and S. H. Gellman, *J. Am. Chem. Soc.* **112**, 6732-6734 (1990).
 8. L. S. W. L. Sokol, L. A. Ochrymowycz, and D. R. Rorabacher, *Inorg. Chem.* 3189-95 (1981).
 9. J. M. Desper and S. H. Gellman, *J. Am. Chem. Soc.*, **113**, 704-6 (1991).
 10. S. R. Cooper, *Acc. Chem. Res.*, **21**, 141-6 (1988).
 11. M. Micheloni, P. Paoletti, L. L. Sigfried-Hertli, and T. A. Kaden *J. Chem. Soc., Dalton Trans.*, 1169-72 (1985).
 12. L. Siegfried and T. A. Kadan, *Helv. Chim. Acta*, **67**, 29-37 (1984).
 13. H. Gampp, M. Maedel, A. D. Zuberhuhler, and Th. A. Kadan *Tranta*, **27**, 573-84 (1980).
 14. C. J. Broan, J. P. L. Cox, A. S. Craig, R. Katakya, D. Parker, A. Harrison, A. M. Ramdall, and G. Ferguson, *J. Chem. Soc. Perkin Trans. 2*, 87-98 (1991).
 15. H. Tsukube, K. Yamashita, T. Iwachido, and M. Zenki, *Tetrahedron Lett.*, **29**, 569 (1988).
 16. Reed M. Izatt, J. S. Bradshaw, S. A. Nielson, J. D. Lamb, and J. J. Christensen, *Chem. Rev.*, **85**, 271-339 (1985).
 17. M. Kodama E. Kimura, S. Yamakuchi, and *J. Chem. Soc. Dalton Trans.* 2536 (1980).
 18. L. F. Lindoy, The chemistry of Macrocyclic Ligand Complexes Cambridge Univ. Press, New York, NY. 133p. (1989).
 19. N. W. Alcock, K. P. Balakrishnan, and Peter Moor, *J. Chem. Dalton Trans.*, 1743 (1986).
 20. P. K. Chan, D. A. Isabirye, and C. K. Poon, *Inorg. Chem.*, **14**, 2579 (1975).
 21. A. Seminar and A. Musumeci, *Inorg. Chem. Acta.*, **39**, 9 (1980).
 22. W. J. Gear, *Coord. Chem. Rev.*, **7**, 81 (1971).
 23. M. Kodama and E. Kimura, *J. Chem. Soc. Dalton Trans.*, 1473 (1977).
 24. (a) R. Delgado and J. J. R. Frausto Da Silva, *Talanta*, **29**, 815 (1982); (b) D. T. Sawyer and P. J. Paulsen, **30**, 816 (1983).
 25. T. M. Fyles and D. M. Whitfield, *Can. J. Chem.*, **62**, 507 (1984).
 26. Ohjin Jung, Chilnam Choi, and Hakjin Jung, *Bull. Kor. Chem. Soc.*, **12**, 130 (1991).
 27. J. F. Desreux, *Inorg. Chem.*, **19**, 1319 (1980).
 28. H. D. Kim, Ph. D. Thesis. Chosun Univ., Kwangju, Korea (1992).
 29. J. M. Desper and S. H. Gellman, *J. Am. Chem. Soc.*, **112**, 6732 (1990).
 30. D. J. Cram, *Angew. Chem. Int. Ed. Engl.*, **25**, 1039 (1986).
 31. R. J. Pederson, *J. Am. Chem. Soc.*, **85**, 3553 (1963).
 32. K. H. Wong, G. K. Konizer, and J. Smid, *J. Am. Chem. Soc.*, **92**, 666 (1970).

Electrochemical Behavior of Mordant Red 19 and its Complexes with Light Lanthanides

Sang Kwon Lee, Taek Dong Chung, Song-Ju Lee[†], Ki-Hyung Chjo[†],
Young Gu Ha, Ki-Won Cha[‡], and Hasuck Kim*

Department of Chemistry, Seoul National University, Seoul 151-740

[†]*Department of Chemistry, Chonnam National University, Kwangju 500-757*

[‡]*Department of Chemistry, Inha University, Incheon 401-751. Received March 4, 1993*

Mordant Red 19(MR19) is reduced at mercury electrode at -0.67 V vs. Ag/AgCl with two electrons per molecule in pH 9.2 buffer by differential pulse polarography and linear sweep voltammetry. The peak potential is dependent on the pH of solution. The exhaustive electrolysis, however, gives 4 electrons per molecule because of the disproportionation of the unstable hydrazo intermediate. The electrochemical reduction of lanthanide-MR19 complexes is observed at more cathodic potential than that of free ligand. The difference in peak potentials between complex and free ligand varies from 75 mV for La³⁺ to 165 mV for Tb³⁺ and increases with increasing the atomic number of lanthanide. The electrochemical reduction of lanthanide complexes with MR19 is due to the reduction of ligand itself, and it can be potentially useful as an indirect method for the determination of lanthanides. The shape of *i*-E curves and the scan rate dependence indicates the presence of adsorption and the adsorption was confirmed by potential double-step chronocoulometry and the effect of standing time. Also the surface excess of the adsorbed species and diffusion coefficients are determined. The composition of the complex is determined to be 1:2 by spectrophotometric and electrochemical methods.

Introduction

Very similar electronic structure of lanthanides makes it difficult to separate one lanthanide from the others. The de-

velopment of simple and effective method of separation is still one of the challenging subjects in this field. The direct electrochemical reduction of lanthanides in aqueous media occurs at so negative potentials that hydrogen evolution in-

terferes with the lanthanide's reduction even at mercury except Sm^{3+} , Eu^{3+} , and Yb^{3+} . Therefore, electrochemical studies of catalytic and adsorptive wave using various ligands (triphenylmethane dyes², hydroxyazo dyes³⁻⁷, macrocyclic compounds such as tetracycline⁸, crown ether⁹, cryptand¹⁰, and dipthalocyanine¹¹, and EDTA analogue¹²), which are known to form stable complexes with lanthanides, have been reported.

Willard and Dean³ have first observed the split of polarographic wave when Al^{3+} ion is added to azo dye solution, Eriochrome Violet B (or Solochrome Violet RS, Mordant Violet 5). Florence and Aylward⁵ have shown that lanthanides form 1:2 complexes with Eriochrome Violet B, and that the potential difference between ligand and complex waves increased from 45 mV (La^{3+}) to 234 mV (Lu^{3+}) with increasing the atomic number of lanthanide. Palmer and Reynolds⁶ studied on the complex wave of the above dye with metal ions such as Al^{3+} and La^{3+} for analysis and reported that the detection limit was 0.5-10 $\mu\text{g/ml}$ in pH 13 buffer solution containing piperidine. Thakur and Waters⁷ have proposed a method for the analysis of Gd^{3+} using Solochrome Violet RS with fast sweep cathode ray polarography in 0.1 M KCl.

With triphenylmethane dyes, Zhang and Gao² have examined the waves of light rare earth elements in the presence of *o*-cresolphthalexon by single sweep polarography. They have reported the reduction potential of adsorptive complex wave is more negative than that of free ligand and the peak height of the complex is proportional to the concentration of lanthanide ions in the range of 10^{-5} M to 10^{-7} M. Also they have found that the adsorptive complex wave appears at very near the wave of ligand itself when thymolphthalexon is used instead, and the reduction current of free ligand decreases with increasing the concentration of metal ion.

These results prompt us to find other electrochemically active ligands which can be used to form stable complexes with lanthanides. Three such ligands have been found and it is shown that they can be used for the indirect determination of lanthanides¹³. Among these ligands, we are reporting on the electrochemical properties of Mordant Red 19 which is one of hydroxyazo dyes and its lanthanide complexes.

Experimental Section

Apparatus. An EG&G-PAR 174A Polarographic Analyzer and an EG&G-PAR 303 Static Mercury Drop Electrode (SMDE, area=1.6-1.7 cm^2) were used for dc and differential pulse polarography. Three-electrode system in electrochemical measurement with hanging mercury drop (HMDE) as working electrode, platinum wire (0.5 mm diameter) as counter electrode, and silver-silver chloride (Ag/AgCl/sat'd KCl) as reference electrode were used. Most of the data were recorded on a BD91 X-Y recorder (Kipp and Zonen Co., Netherlands).

A BAS-100A electrochemical analyzer (Bioanalytical Systems, Inc., W. Lafayette, IN, U. S. A.) was used for cyclic voltammetry (CV), linear sweep voltammetry (LSV), and chronocoulometry (CC). All measurements were performed at $25 \pm 0.2^\circ\text{C}$.

Nitrogen gas purified by passing through vanadous(II) solution was bubbled to deaerate the solution. For potentiostatic bulk electrolysis, a mercury pool was used as a working

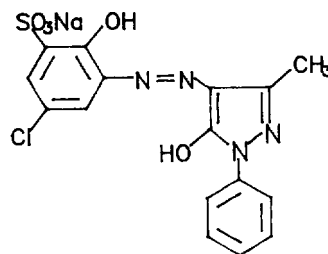


Figure 1. Structure of Mordant Red 19.

electrode. The absorption spectra of the ligand and complexes were obtained with a Beckman DU64 UV/Visible spectrophotometer.

Reagents. Mordant Red 19 (MR19) was purchased from Aldrich and used as received. The pH of the solution was maintained with Clark-Lubs buffer for pH 1.6, 6.6-7.1, with acetic acid buffer for pH 3.2-6.1, and with ammonia buffer for pH 8.3-10.5. 0.1 M NaCl was added as supporting electrolyte. All the chemicals were GR grade. The calculated amount of dried lanthanide oxides (>99.5% purity) was weighed and dissolved in small quantity of concentrated HCl, then diluted with de-ionized and distilled water to make stock solutions of 1.0×10^{-3} M.

Results and Discussion

Electrochemical Behavior of MR19. MR19(5-hydroxy-3-methyl-1-phenyl-4[(5-chloro-2-hydroxy-3-sulfophenyl)-azo]-pyrazole, sodium salt) has two electrochemically reducible groups, one is azo group and the other is chloro group, and its structure is shown in Figure 1. Differential pulse polarogram (DPP) of 1.0×10^{-4} M MR19 buffered at pH 9.2 in 0.1 M NaCl is shown in Figure 2a. A large and sharp reduction peak is observed at -0.665 V. Also very similar shape of linear sweep polarogram is shown in Figure 2b. The reduction of chloro functional group in the formula is ruled out because the observed potential is less cathodic than the values generally observed with chloroazobenzenes (< -1.7 V)¹⁴. Also this presumption is acceptable since the color of solution fades away during bulk electrolysis and becomes colorless. The color must be sustained if chloro group is involved in the reduction.

The dc polarogram at pH 9.2 shows as if a polarographic maximum exists and the shape is not affected even with 0.1 ml of 0.002% Triton X-100. It turns out that this maximum is due to the adsorption of the ligand, and the excess amount of surfactant removes all the polarographic wave. The number of electrons involved in the reduction is estimated from the diffusion limiting current. It is 1.7 when the diffusion coefficient is taken as 1.0×10^{-5} cm^2/sec or 2.4 with $D = 5 \times 10^{-6}$ cm^2/sec (see the chronocoulometry section). It is, therefore, reasonable to take as $n=2$ for the reduction of MR19.

Another way to get the number of electrons is by taking the diffusion limiting current at various drop times such as 0.5, 1, 2 and 5 sec, and plot them against $t^{-1/2}$. From the slope of 7.2×10^{-7} $\text{A} \cdot \text{sec}^{1/2}$, it is reasonable to take the number of electrons as two with the diffusion coefficient of 1.6×10^{-5} cm^2/sec according to the Cottrell equation. Also the number of electrons involved can be confirmed from the peak width of DPP. The full width of the peak at half height

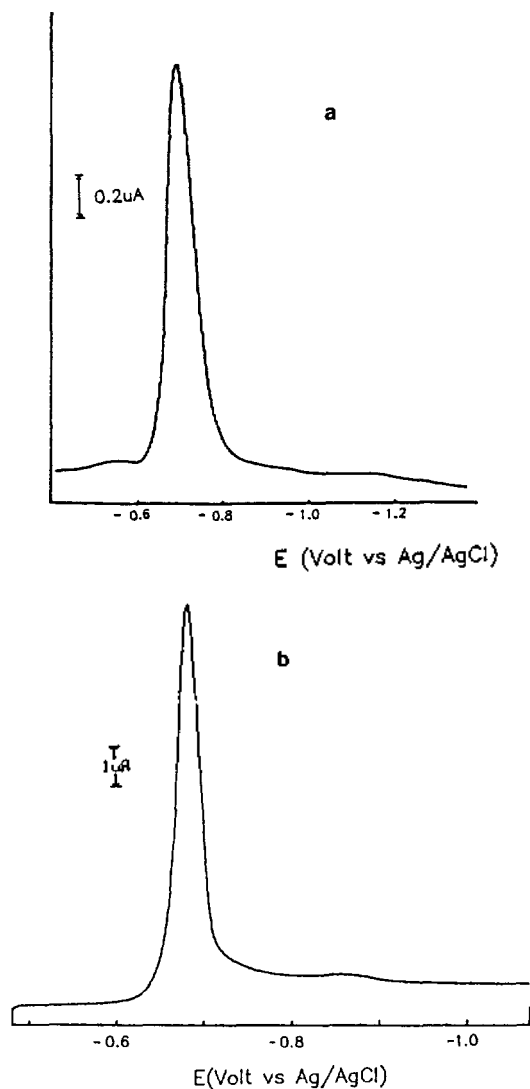


Figure 2. (a) Differential pulse polarogram of MR19. drop time = 2 sec, scan rate = 5 mV/sec, and pulse amplitude = 10 mV. (b) linear sweep voltammogram of MR19. scan rate = 100 mV/sec, electrolyte; 0.1 M NaCl, pH 9.2, [MR19] = 1.0×10^{-4} M.

is expressed as $W_{1/2} = 3.52RT/nF^{15}$. The experimentally measured $W_{1/2}$ values are 52.5-65 mV in our case, while the calculated value for $n=2$ is 45.2 mV at 25°C. Generally, the observed peaks are wider because of the finite width of pulse used in the measurement.

These n values of two is in good agreement with the previous report for dihydroxyazo compound¹⁶ which has the basically similar structure. Therefore, two protons in addition to two electrons must be involved in the reduction since the half wave potential above pH 8.2 shifts to cathodic direction by 50-60 mV/pH (region e in Figure 3).

The peak potential is determined to be dependent on the pH of the medium. As shown in Figure 3, the pH dependence of the electrochemical reduction indicates the reaction is a complicated one and it can be divided into 5 regions, a through e. The peak potential shifts about 50-60 mV/pH in the regions a, c and e which is typical behavior for the reaction with same number of electrons and protons, while two regions, b and d show little pH dependence. This means

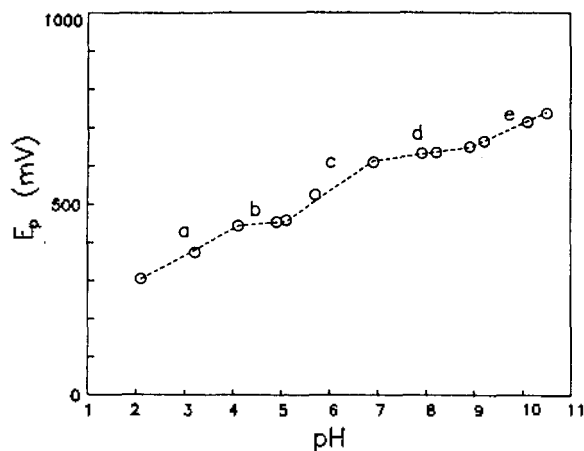


Figure 3. pH Dependence of peak potential of MR19.

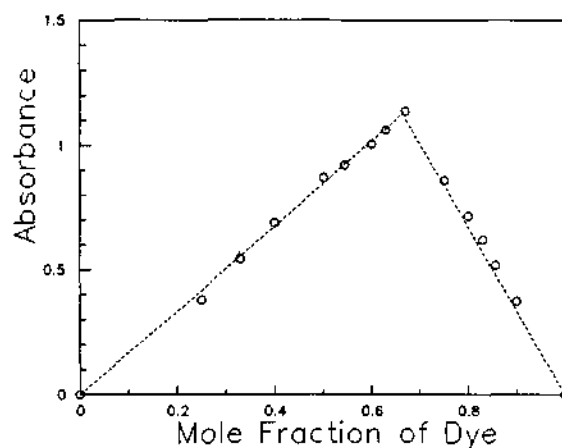


Figure 4. Results of continuous variation plot.

The absorbance values are corrected for free ligand after complexation because ligand also absorbs appreciably at λ_{max} (complex) = 458 nm. $[La^{3+}] + [MR19] = 1.0 \times 10^{-4}$ M.

that no proton is involved in the reduction in these two pH regions.

MR19 does not produce any oxidation wave in the reverse scan of cyclic voltammetry and the cathodic peak potential shifts to negative direction with increasing the scan rate as it evidences in a totally irreversible case.

Stoichiometric Composition of Complex. In order to determine the stoichiometry of the complex, spectroscopic measurement is made with La^{3+} and MR19. The λ_{max} of La^{3+} -MR19 complex appears at 458 nm with $\epsilon = 33,500$, while that of MR19 is 470 nm with $\epsilon = 13,200$. Figure 4 shows the result of continuous variation method. A maximum absorbance is observed where the mole fraction of MR19 is about 0.67, so the composition of La^{3+} -MR19 complex must be 1 : 2. All the absorbances are corrected for free ligand after complexation because the ligand and complex absorb appreciably at 458 nm. This result is in good agreement with the report made by Coates and Rigg¹⁷ who have shown that di-*o*-hydroxyazo dye (Eriochrome Violet B) forms 1 : 2 complex with Cr^{3+} .

Electrochemical Properties of MR19-Lanthanide Complexes. Linear sweep polarograms with solution containing 5.0×10^{-5} M Gd^{3+} and 1.0×10^{-4} M MR19 in pH

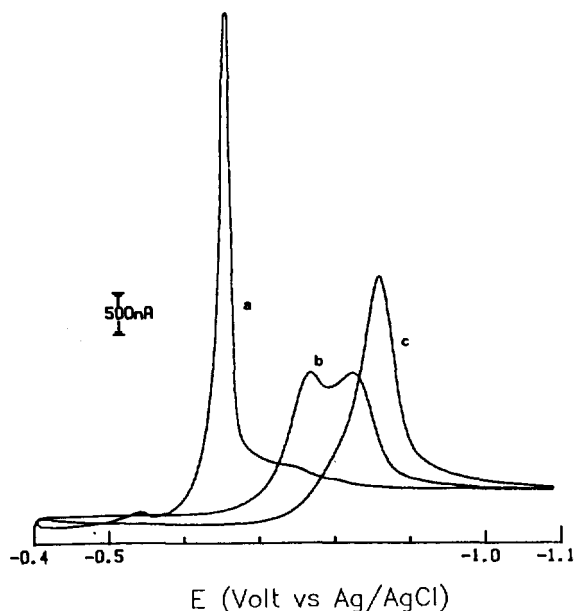


Figure 5. Linear sweep voltammograms of Gd^{3+} -MR19 at different pH. (a) pH 7.3, (b) pH 8.2, (c) pH 9.2. $[Gd^{3+}] = 5.0 \times 10^{-5}$ M, $[MR19] = 1.0 \times 10^{-4}$ M, and $A = 1.6 \times 10^{-2}$ cm.

7.3, 8.2 and 9.2 provide useful information on complexation. In pH 7.3 (Figure 5a), a sharp reduction peak of MR19 appears at -0.64 V and a very small shoulder wave at -0.75 V. Here i_p is $5.83 \mu A$ while i_p of free ligand itself without Gd^{3+} is $5.88 \mu A$. Therefore, almost no complex is considered formed at this pH. In pH 8.2, two splitted complex peaks near -0.77 V and -0.82 V are observed (Figure 5b) while a sharp peak of MR19 is observable at -0.69 V with solution without any metal ion. Since the reduction peak of free ligand is not observed, complexation seems complete at pH of 8.2. It is not clear at this point why two peaks are observed at this pH. One of the peaks, however, corresponds to the potential where the complex peak is located in pH 9.2. A large single peak was observed at -0.86 V when pH was 9.2 (Figure 5c). These results suggest that lanthanide ions can form stable respective complexes with MR19 at pH higher than 8.2, and that the peak potential of complex shifts toward cathodic direction with increasing value of pH like MR19. Since a single reduction peak is simpler to interpret the experimental data, most of experiments are performed at pH value of 9.2.

Single sweep polarography was employed as an analytical technique for adsorptive complex wave by Zhang and Gao². This method is particularly suitable in the case of fast adsorption, where rapid scanning can be made after a short equilibration of about several seconds. Figure 6 illustrates fast linear sweep polarograms of complexes of La^{3+} (Figure 6a) and Tb^{3+} (Figure 6b). The differences in two peak potentials between free ligand and its metal complex are 75 mV for La^{3+} and 165 mV for Tb^{3+} . Similar potential shifts are also observed in DPP as shown in Table 1.

Table 1 shows the result of the electrochemical behavior of MR19-lanthanide complexes. The difference in peak potentials between free ligand and complex depends on the lanthanides used in complexation. It seems ΔE_p is increasing with increasing the atomic number. This trend is opposite

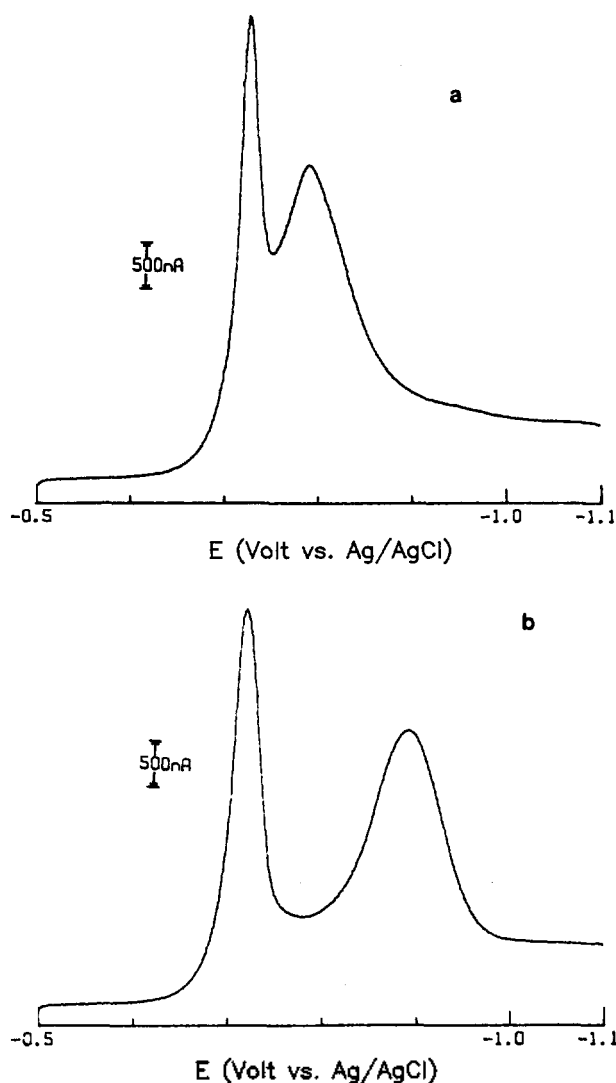


Figure 6. Linear sweep polarograms of complex. (a) La^{3+} -MR19, (b) Tb^{3+} -MR19, Concentration = 1.0×10^{-5} M, Electrolyte: 0.1 M NH_3-NH_4Cl , pH 9.2, $A = 1.6 \times 10^{-2}$ cm², Scan Rate = 300 mV/sec.

Table 1. Peak Potentials of MR19 and Lanthanide-MR19 Complexes by DPP

Element	Ligand		Complex	
	$-E_p$, mV ^a	$-E_p$, mV ^a	$-E_p$, mV ^a	ΔE_p , mV
La	665	740	740	75
Pr	670	776	776	106
Sm	667	794	794	127
Eu	670	810	810	140
Gd	670	820	820	150
Tb	673	838	838	165

^avs. Ag/AgCl/sat'd KCl. Solution: 1.0×10^{-4} M MR19 + 1.0×10^{-5} M lanthanide pH=9.2, Drop time=2 sec, Scan Rate=5 mV/sec, and Pulse amplitude=10 mV.

to the Zhang's result² in the case of *o*-cresolphthalexon which is one of triphenylmethane dyes. But it is similar to that of Solochrome Violet RS^{5,18} which is a dihydroxyazo dye

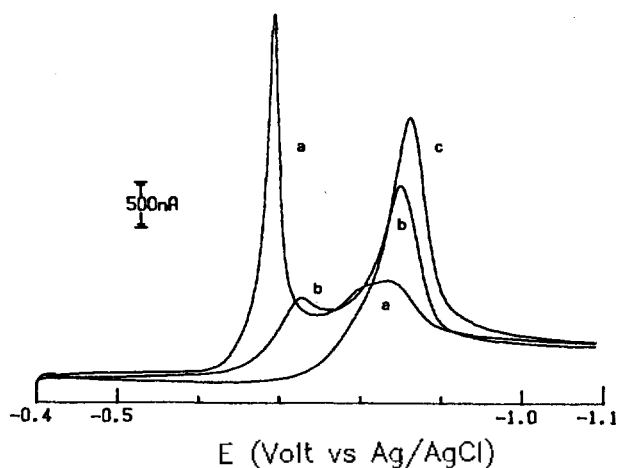


Figure 7. Linear sweep voltammograms of Gd^{3+} -MR19 complex at pH 9.2. The concentration of MR19 is fixed at 1.0×10^{-4} M and the concentrations of Gd^{3+} are (a) 5.0×10^{-6} M, (b) 1.0×10^{-5} M, and (c) 5.0×10^{-5} M. Scan Rate = 100 mV/sec and $A = 1.6 \times 10^{-2}$ cm^2 .

like MR19 used in this investigation. Since the shift of peak potential depends on the concentration of ligand and on the formation constant of complexes, a bigger potential shift implies a larger formation constant. This means the complex of heavier lanthanide ions must be more stable than those of lighter lanthanides in the case of hydroxyazo ligand. Therefore this kind of stability indicates that there must be no steric hindrance involved in the case of MR19 to form complexes with metals of decreasing ionic size (increasing the atomic number), and that some contributions from 4f electrons must be existed. The difference in peak potential is very useful to distinguish one lanthanide from the others in a mixture of selected ions. Spectroscopic techniques such as emission or absorption generally are not very selective to identify one from the others.

A possible analytical aspect is noticed when the peak height of MR19 gradually decreases as the concentration of lanthanide ion increased by DPP when the concentration of MR19 is fixed at 1.0×10^{-4} M. Then, MR19's peak disappears completely when the molar ratio of lanthanide to MR19 reaches to 1:2. Further increase of lanthanide ion concentration does not give any effect on the peak height of complex. Therefore, 1:2 complexation is also confirmed electrochemically. Either the decrease of the peak height of ligand or the increase of that of complex can be utilized as an analytical application which point will be published in detail in a separate paper.

Linear sweep polarograms obtained at pH 9.2 from the solution containing 1.0×10^{-4} M-MR19 with varying concentration of Gd^{3+} also confirms the above mentioned stoichiometry. If the concentration of lanthanide ion is low, two peaks at -0.68 V and -0.83 V are observed due to the presence of free ligand and its complex, respectively. Only a single peak, however, is obtained at -0.86 V when the concentration of Gd^{3+} is more than a half of that of ligand. And the peak current of the complex after this point is independent of the concentration of Gd^{3+} . The complex wave does not produce any oxidation peak, therefore, the electrochemical reduction of the complex proceeds irreversibly like

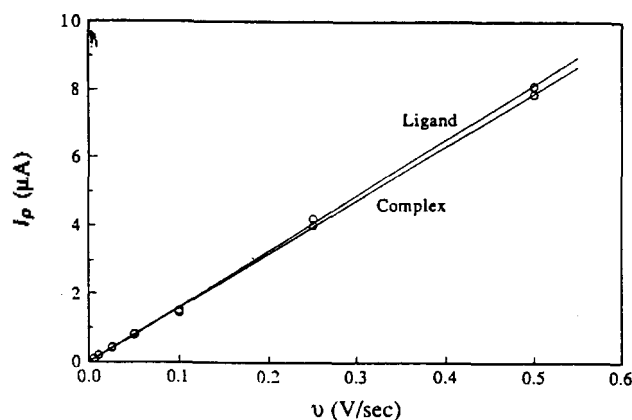


Figure 8. Scan rate dependence of peak current. Concentrations of the solution from the adsorbed layers are made are 1.0×10^{-4} M MR19 and 5.0×10^{-5} M Gd^{3+} -MR19. See the text for details.

Table 2. Charges Obtained from Peak Area of the Cyclic Voltammograms of Adsorbed Layers^a

Scan rate mV/sec	Ligand ^b μC	Complex ^c μC
1	1.09	1.43
5	1.10	1.45
50	1.09	1.51
100	1.08	1.41
200	1.08	1.41

^aAdsorbed layers were obtained by soaking a fresh mercury drop in each solution for 30 sec. then the mercury drop was washed with buffer solution (pH=9.2) before linear scan in the solution containing only buffer and supporting electrolyte. ^bObtained with 1.0×10^{-4} M MR19 solution. ^cObtained with 5.0×10^{-5} M Gd^{3+} -MR19 solution. $E_i = -0.5$ V, Scan Rate = 100 mV/s, $A = 1.6 \times 10^{-2}$ cm^2 , and pH=9.2.

the ligand itself.

Adsorption Behavior of Complex

Effect of Scan Rate. The scan rate dependence for the solution containing either 1.0×10^{-4} M-MR19 or 1.0×10^{-4} M-MR19 and 5.0×10^{-5} M Gd^{3+} in pH of 9.2 shows an intermediate value between a half power and one to the scan rate. This implies that some diffusion process in addition to surface process is involved in the reduction. In order to simplify the situation, a mercury drop (HMDE) is placed in the solution containing either ligand or ligand with lanthanide ion for 30-60 sec which is determined to be long enough to reach a complete coverage. Then the mercury drop is washed thoroughly with the same pH buffer and is placed again in the buffer solution without ligand nor complex for linear scan experiment. The shape of the peak in both cases is very sharp, especially in the case of ligand as shown in Figures 6 and 7, and the current value returns to the residual level. Figure 8 illustrates the linear scan rate dependence for ligand and Gd^{3+} -MR19 complex. I_p must be proportional to $v^{1/2}$ in the diffusion controlled process according to Randles-Sevcik equation¹⁹, and directly proportional to v in the surface phenomena²⁰. Based on the wave shape and the scan rate dependence, the current is due to the diffusion

Table 3. Effect of Standing Time on the Peak Height and Peak Potential from the Bulk Solution

Time (sec)	Ligand		Complex	
	i_p (μA)	$-E_p$ (mV)	i_p (μA)	$-E_p$ (mV)
0	7.35	651	3.04	817
5	8.80	657	3.30	820
10	10.17	666	3.38	822
20	12.08	680	3.55	825
30	13.83	688	3.66	827
60	15.31	705	3.88	831
90	15.87	710	3.98	836
120	16.30	713	4.05	839
180	16.43	714	4.18	844

$E_i = -0.4$ V, Scan rate = 100 mV/s, $A = 1.7 \times 10^{-2}$ cm², pH = 9.2. Solutions are 1.0×10^{-4} M MR19 and 5.0×10^{-5} M Tb³⁺-MR19 for ligand and complex, respectively.

from bulk and to the adsorbed species on the electrode.

The charges by integrating the peak at different scan rate are shown in Table 2. The amount of charge is about 1.45 μC for complex regardless of the scan rate, which is equivalent to 3.65×10^{-12} mol adsorbed on a mercury drop. Since 2 electrons are required to reduce each ligand molecule, $n=4$ was taken in the above calculation. For MR19, the integration give 1.08 μC , so the quantity adsorbed is calculated as 5.6×10^{-12} mol assuming $n=2$. These quantities are very close to what one expects from a monolayer of molecules covers the whole mercury drop. The amount of charge due to the adsorbed complex is not exactly one half of that of the ligand because the cross sectional area of complex is not twice of that of the ligand considering its structure.

Since the monolayer covers the electrode with the thickness in the order of several Å, we can imagine this situation as thin layer electrochemistry case where all the electrochemically active species exist at the electrode. The observed peak current by linear sweep voltammetry for the irreversible case is $i_p = n\alpha n_a F^2 v VC^* / (2.718RT)$ where v is the scan rate and VC^* is the quantity being electrolyzed. The $n\alpha n_a$ value calculated from the above equation is 1.4 and therefore, n must be 2 since αn_a is generally close to 0.5. This is again in good agreement with the result obtained from the Cottrell plot.

Effect of standing time. According to Koryta²¹, the fractional coverage of electrode surface is proportional to the square root of the ratio of standing time (τ) to complete coverage time (T), $\Theta \propto (\tau T)^{1/2}$. This means that fractional coverage increases very rapidly at the beginning of standing time and then increases slowly until complete coverage is established. The higher the concentration of adsorptive species, the shorter the time is needed to reach a complete coverage. In order to find out how fast MR19 and its lanthanide complex adsorb at mercury, BAS-100A and SMDE are connected, and linear sweep polarograms are obtained with scan rate of 100 mV/sec with varying standing time (Table 3). Indeed, in the beginning of the standing time (for example when τ is a few second, where potential scan is activated immediately after the fresh electrode is immersed into the solution),

Table 4. Effect of Standing Time to form the Adsorbed Layers

Time (sec)	Ligand		Complex	
	i_p (μA)	$-E_p$ (mV)	$-i_p$ (μA)	$-E_p$ (mV)
5	1.33	740	1.46	854
10	1.20	744	1.19	881
20	1.24	733	1.64	846
30	1.44	736	1.71	843
60	1.40	732	1.42	877
90	1.70	719	1.36	872
120	1.55	727	—	—

$E_i = -0.4$ V, Scan rate = 100 mV/s, $A = 1.7 \times 10^{-2}$ cm², and pH = 9.2. Solutions are 1.0×10^{-4} M-MR19 and 5.0×10^{-5} M Tb³⁺-MR19 for ligand and complex, respectively. Adsorbed layers were obtained by soaking a fresh mercury drop in each solution for 30 sec, then washed with buffer solution (pH = 9.2) before linear scan in the solution containing only buffer and supporting electrolyte.

Table 5. The Surface Excess by Chronocoulometry

τ (msec)	Surface excess		Diffusion coefficient	
	($\times 10^{-10}$ mol/cm ²)		($\times 10^{-5}$ cm ² /sec)	
	MR19	Gd-MR19	MR19	Gd-MR19
25	3.35	1.62	1.7	—
50	3.25	1.53	1.4	0.7
100	3.18	1.41	1.6	1.1
250	2.96	1.21	2.0	1.3
500	2.59	—	2.5	1.7

$A = 1.7 \times 10^{-2}$ cm², $E_i = -0.4$ V, $E_f = -1.2$ V. Solution: 1.0×10^{-4} M-MR19 and 5.0×10^{-5} M Gd-MR19 in pH 9.2.

the observed peak height is about 40-70% of the one with a longer period of adsorption. The time needed to reach an equilibrium of adsorption is around 30-60 sec at pH 9.2 for both free ligand and complex. In this experiment, current came not only from the adsorbed species but also from the bulk solution by diffusion.

Instead of performing the experiment in the bulk solution, linear scan polarograms are obtained with only adsorbed layers on the mercury drop as before. The peak current is about 1.5 μA for MR19 and 1.7 μA for complex regardless of standing time for adsorption from 5 to 120 sec (Table 4). This result again strongly indicates that the adsorption process is very fast.

Chronocoulometry. Table 5 shows the surface excesses and diffusion coefficients obtained from the bulk solution by chronocoulometry where potential pulses are applied from -0.4 V to -1.2 V for 25 to 500 msec. Surface excess is calculated from the intercept of Anson plot²², and the quantity of MR19 adsorbed is determined to be 5.4×10^{-12} mol (3.2×10^{-10} mol/cm²), and that of Gd³⁺-MR19 is 2.6×10^{-12} mol (1.5×10^{-10} mol/cm²). These results agree reasonably well with the values obtained from the LSV experiment.

Considering the molecular size of MR19 as about 8 Å,

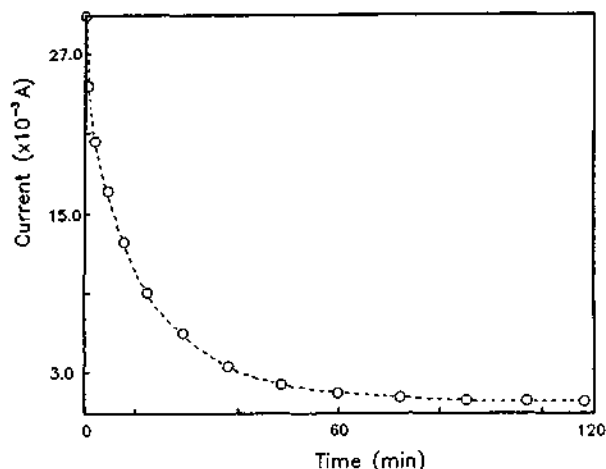


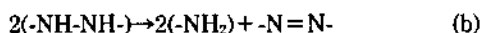
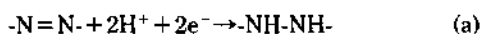
Figure 9. Current-time curve for the reduction of Gd^{3+} -MR19 complex by coulometry, pH=9.2, $E = -1.20$ V (vs. Ag/AgCl/sat'd KCl), and Concentration of Complex = 2.5×10^{-6} M.

2.0×10^{14} molecules can be existed in each cm^2 if a monolayer coverage is realized, and the quantity of adsorbed species is about 3.3×10^{-10} mol/ cm^2 . Again, the amount of species possibly adsorbed on mercury comes very close to one obtained by chronocoulometry and by integrating the current from linear sweep voltammetry. So our experimental results indicate that the adsorption at mercury electrode occurs as monolayer. Diffusion coefficients calculated from the slope of Anson plot are 1.8×10^{-5} cm^2/sec for MR19 and 1.2×10^{-5} cm^2/sec for MR19-Gd complex.

Bulk Electrolysis. Exhaustive electrolysis is performed to find the number of electrons involved in the electrochemical reduction of MR19 and its lanthanide complex employing a mercury pool as a working electrode. The potential of -1.2 V which is far beyond the reduction potential of complex is applied and the current is monitored throughout the experiment.

Figure 9 shows the variation of current during the electrolysis. A linear relationship between $\log[i(t)/i_0]$ and electrolysis time upto about 3 minutes is observed. Then, serious deviation from the linearity appears beyond 6 minutes. This and the irreversible behavior in cyclic voltammetry imply chemical reactions are involved after electron transfer. It takes almost 2 hours to get a constant residual current. The color of the solution gradually fades as electrolysis proceeds, and it eventually becomes colorless.

The number of electrons calculated from the charge is 8.2 for complex, while that for MR19 is 3.83. These values are almost twice the values we have obtained in previous sections. According to Laitinen¹⁶ and Florence^{18,23}, the reduction path of di-*o*-hydroxyazo involves a potential-determining 2-electron step yielding an unstable hydrazo intermediate which disproportionates to amines and original azo compounds, leading to a total n value of four.



The step (b) proceeds very rapidly in strong acidic condition, while it is slow in basic media. Even at a pH of 9.5, the polarographic wave height corresponds to a little more

than two electrons, while the coulometric measurement indicates four because of the time scale of experiment^{16,24}. Therefore, it is reasonable to get $n=4$ for MR19 and 8 for complex by the coulometric measurement in this study.

Conclusions

A very sharp and large reduction peak is observed at -0.67 V from MR19, a di-*o*-hydroxyazo dye, in pH of 9.2. When the pH is changed in the range from 1.6 to 10.5, a plot of peak potential vs. pH can be divided into 5 regions. The peak potential shifts cathodically by 50-60 mV/pH for pH greater than 8.2, indicating the same number of protons accompanies electrons in the reduction. We find $n=2$ not only from the slope of the Cottrell plot but also from the width of peak at the half height in DPP. The number of electrons obtained from coulometry is two times of those obtained by other techniques because of disproportionation of the product to the original azo compound and amine after 2-electron process. MR19 forms stable 1:2 complexes with lanthanide ions at pH greater than 8.2. We conclude the reduction reaction of ligand and lanthanide complexes proceeds totally irreversibly from cyclic voltammetric results. Since the peak current increases more than square root of the scan rate, the electrochemical process is considered to involve some surface process in addition to diffusion. The quantity of adsorbed molecules for ligand and complex is about the same for one would expect from a monolayer adsorption by chronocoulometry. Diffusion coefficients obtained are 1.8×10^{-5} cm^2/sec and 1.2×10^{-5} cm^2/sec for MR19 and Gd^{3+} -MR19, respectively.

The reduction of complex appears at more cathodic potential than that of free ligand. Since the difference between peak potentials of ligand and complexes increases with increasing the atomic number of lanthanide, it can be possible to analyze them selectively with electrochemical methods.

Acknowledgment. This work was supported in part by the Ministry of Education of the Republic of Korea through the Basic Science Research Institute Program (1990) and by the KOSEF (89-03-12-04). Also one of authors (SL) expresses sincere thanks to the Korea Research Foundation providing for one year fellowship to participate in this work.

References

1. E. Steeman, E. Temmerman, and F. Verbeek, *J. Electroanal. Chem.*, **89**, 97-113 (1978).
2. M. Zhang and X. Gao, *Anal. Chem.*, **56**, 1912-1917 (1984).
3. H. H. Willard and J. A. Dean, *Anal. Chem.*, **22**, 1264 (1950).
4. S. W. Kim, J. H. Jang, M. Y. Seo, and L. M. Doh, *Proceedings of the Basic Science Research Institute*, **4**, 153-162 (1990).
5. T. M. Florence and G. H. Aylward, *Aust. J. Chem.*, **15**, 65 (1962).
6. S. M. Palmer and G. F. Reynolds, *Z. Anal. Chem.*, **216**, 202 (1966).
7. M. L. Thakur and S. L. Waters, *J. Inorg. Nucl. Chem.*, **35**, 1787 (1973).
8. X. Z. Ye and X. Gao, *Chinese J. Rare Earth*, **3**, 77 (1985).
9. J. Massaux, J. Desreux, C. Chambre, and G. Duyckaerts,

- Inorg. Chem.*, **19**, 1893 (1980).
10. C. Hall, N. Sharpe, I. Danks, and Y. Sang, *J. Chem. Soc. Chem. Comm.*, 419 (1989).
 11. M. Piou and C. Clarisse, *J. Electroanal. Chem.*, **249**, 181 (1988).
 12. Si Soon Lee and Ku Soon Chung, *Abstracts of the 68th KCS Annual Meeting*, FBunF12Ku, p. 142 (1991).
 13. Hasuck Kim and Sang Kwon Lee, *Bull. Kor. Chem. Soc.*, **14**, 165 (1993).
 14. A. J. Bard and H. Lund, *Encyclopedia of Electrochemistry of the Elements*, Vol. XIII, Marcel Dekker, Inc., New York, Chap. 4 (1978).
 15. A. J. Bard and Faulkner, "Electrochemical Methods", Wiley, New York, p. 195 (1980).
 16. H. A. Laitinen and T. J. Kneip, *J. Am. Chem. Soc.*, **78**, 736 (1956).
 17. E. Coates and B. Rigg, *Trans. Faraday Soc.*, **58**, 1 (1962).
 18. T. M. Florence and W. L. Belew, *J. Electroanal. Chem.*, **21**, 157 (1969).
 19. (a) J. E. B. Randles, *Trans. Faraday Soc.*, **44**, 327 (1948); (b) A. Sevcik, *Collect. Czech. Chem. Commun.*, **13**, 349 (1948).
 20. R. H. Wopschall and I. Shain, *Anal. Chem.*, **39**, 1514 (1967).
 21. J. Koryta, *Collect. Czech. Chem. Commun.*, **18**, 206 (1953).
 22. p. 537 of reference 15.
 23. T. M. Florence, *Aust. J. Chem.*, **18**, 619 (1965).
 24. T. M. Florence and G. H. Aylward, *Aust. J. Chem.*, **15**, 416 (1962).

Application of Laser Induced Photoacoustic Spectroscopy in the Investigation of Interaction of Neodymium(III) with Water Soluble Synthetic Polymer

Tae Hyun Yoon, Hichung Moon, Seung Min Park[†], Joong Gill Choi[‡]
and Paul Joe Chong^{*}

Department of Chemistry, Korea Advanced Institute of Science and Technology, Taejon 305-701

[†]*Department of Chemistry, Kyunghee University, Seoul 130-701*

[‡]*Department of Chemistry, Yonsei University, Seoul 120-749*

^{*}*Korea Research Institute of Chemical Technology, P.O. Box 9,
Daeduck Science Town, Taejon 305-606. Received March 30, 1993*

Laser-induced photoacoustic spectroscopy (LIPAS), which utilizes the photothermal effect that results from nonradiative relaxation of excited state molecules, was used in the speciation analysis of the complexes of neodymium(III) and water soluble synthetic polyelectrolyte, poly methacrylic acid (PMAA), in 0.1 M NaClO₄ at pH of 6.0. The minimum detection limit of Nd(III) by LIPAS was 5.0×10^{-6} M. Experiment was carried out at low concentration ratio of Nd(III) to PMAA to assure that 1:1 complexes predominate. The bound and free Nd(III) species were characterized by measuring nonradiative relaxation energy of the excited states (²G_{7/2} and ⁴G_{5/2}) to the metastable state (⁴F_{3/2}). Two species were quantified by deconvolution of the mixed spectrum using their respective reference spectra. The conditional stability constant measured by LIPAS was 5.52 L·mol⁻¹.

Introduction

The migrational behaviours of trivalent lanthanide or actinide ions in a natural environment are determined by their solubility, complex formation, and colloid generation. The complexation of these trivalent ions with naturally occurring organic polyelectrolyte ligands (e.g., humic substances) has been investigated using a number of different methods. The separation methods used include equilibrium dialysis,¹ gel filtration,² and ultrafiltration technique.³ There are many problems associated with the use of separation methods and they are: (1) the labile species can be lost by adsorption on membrane and other materials, (2) chemical equilibria may shift during the separation stage, and (3) low molecular weight complexes may pass through membranes. The nonse-

paration methods such as ISE (ion selective electrode) and conventional absorption spectroscopy are generally preferred, since fewer experimental difficulties are encountered. Even so, obtaining a reliable data is a difficult task, since the polyelectrolyte bound metal concentration is usually calculated as the difference between the total metal and free metal ion concentrations, and they may both be very large numbers. Furthermore, the ion selective electrode can be applied to only a few elements, and due to the low solubility of the trivalent ions (often less than 10⁻⁶ mol·L⁻¹), the speciation analysis using the conventional absorption spectrophotometers poses many challenges, especially when the fingerprint characteristics of weak *f-f* transitions are exploited to identify metal complexes.

More recently, modern spectroscopic methods of high sen-